



Electrospun Mats: From White to Transparent with a Drop

Jonathan Cimadoro, Laura Ribba, Silvia Ledesma, and Silvia Goyanes*

In this article, the transparency of hydrophilic electrospun mats is studied. Results showing how transmittance varies under the action of water are presented. It is observed that swelling plays a crucial role in the transmittance of the material, changing it from opaque to transparent when it is wet. Atomic force microscope measurements show that the diameter distribution of nanofibers is modified during both the wetting and the drying of the mats. Using these distributions and modeling the change in the relative refractive index as a composite material, a qualitative explanation of the mat scattering behavior by using the Mie scattering theory for cylinders has been done. The obtained results indicate that changes on the optical response produced by water contact are different according to the mat thickness: samples with smaller thicknesses can act as a water sensor with a persistent response over time, while samples with thicknesses greater than 7 μm can act as sensors for drying time.

Different mats composed of nanometric fibers can be manufactured by the electrospinning technique. Their versatility allows them to be useful for a huge variety of applications, from medical physics to environmental remediation.^[1,2] In the optical field, electrospun nanofibers were used, for example, for light confinement and propagation and light-coupling devices, due to its subwavelength diameters.^[3–6] Other possible application in this field is the performance of light-emitting mats (from single photon emitters to random cavity lasing) and optical self-waveguides, through the incorporation of fluorescent dyes or semiconductors within nanofibers.^[7,8]

An effect of the nanostructure is that even a transparent polymer could generate a white mat, as a consequence of the

multiple light scattering induced in the nanofibers scaffold. This effect has also been studied in natural nanostructures such as white beetle scales.^[9,10] Taking advantage of this phenomenon and the wide surface area, nanofibers functionalized by metal nanostructures and particles are exploited as effective flexible substrates for enhanced Raman scattering (SERS) analysis.^[11]

Chang et al. showed that the scattering bands of poly(methyl methacrylate) nanofibers were linearly proportional to their diameter, which shows good agreement with a scattering model based on the Mie theory.^[12]

It is also known that, after solvent swelling, the material that forms a polymeric nanostructure becomes a mixture of polymer with solvent. The amount of absorbed solvent is strongly dependent on its affinity with the polymer. Then, optical properties of electrospun mats change when they are put into contact with solvents, due to modifications in nanofiber diameter and relative refractive index.

The swelling effect of polymer mats has been used for several applications, such as the development of vapor sensors.^[13–15] However, there are no works that show how swelling affects the light scattering behavior of electrospun mats producing changes in the material transparency that could remain for several days. Besides, these changes have not been studied through any theoretical model.

The aim of this work is to study the drastic increase in the transmittance produced when an opaque electrospun mat is put into contact with water. The Bashkatova et al. approximation for the scattering of cylindrical particles (in the context of Mie model), is used to obtain a qualitative explanation of this behavior.^[16] Moreover, the transmittance dependence on the mat thickness and the drying time is explored. For this purpose, polyvinyl alcohol (PVA) was used, since it can be electrospun and it is highly sensitive to water, but it is known that after a cross-linking treatment it becomes insoluble.^[17,18] Mats with the smallest thickness, initially opaque, become almost transparent upon wetting and do not become opaque again regardless of the drying time. These samples could be used as water sensors in which the wetting information remains in time, that is, as wetting sensors. On the other hand, mat thicknesses greater than 7 μm show a decrease of the transmittance as the drying time increases. These samples could be used as sensors to give information on how much time passes since the last time they got wet, that is, as drying time sensors.

The UV–vis spectra of the samples were obtained before measuring the transmittance, in order to determine the

J. Cimadoro, Dr. L. Ribba, Dr. S. Goyanes
Universidad de Buenos Aires
Facultad de Ciencias Exactas y Naturales
Departamento de Física
Laboratorio de Polímeros y Materiales Compuestos
Instituto de Física de Buenos Aires–Consejo Nacional de
Investigaciones Científicas y Técnicas (IFIBA-CONICET)
Ciudad Universitaria (1428)
Ciudad Autónoma de Buenos Aires, Argentina
E-mail: goyanes@df.uba.ar

Dr. S. Ledesma
Universidad de Buenos Aires
Facultad de Ciencias Exactas y Naturales
Departamento de Física
Laboratorio de Procesado de Imágenes–Consejo Nacional de
Investigaciones Científicas y Técnicas (LPI-CONICET)
Ciudad Universitaria (1428)
Ciudad Autónoma de Buenos Aires, Argentina

The ORCID identification number(s) for the author(s) of this article can be found under <https://doi.org/10.1002/mame.201800237>.

DOI: 10.1002/mame.201800237

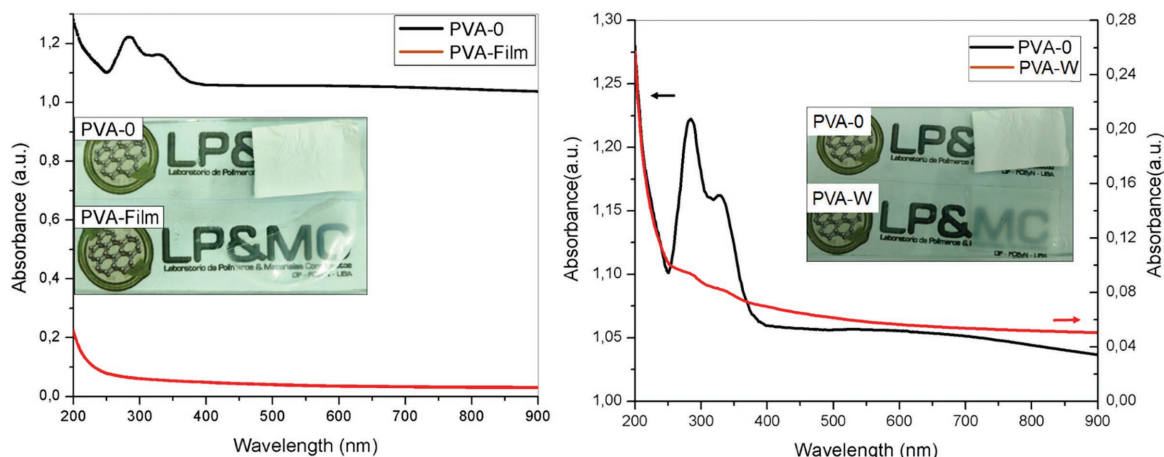


Figure 1. A) UV-vis spectra comparison between mat and continuous film before wetting. B) Comparison of UV-vis mats' response before and after wet. In both figures, photographs of measured samples are included. Samples with 40 μm were used.

wavelength to be used. This should be in the visible spectrum and in an area in which there are no absorption bands, which could be modified with the nanostructure. **Figure 1A** shows UV-vis absorption spectra and the corresponding photographs of an electrospinning mat (PVA-0) and a continuous film (PVA-Film) of the same thickness (40 μm) before wetting. Meanwhile films remained transparent in the region from 400 to 800 nm, the PVA-0 looks white, due to light scattering within the nanostructured material. No changes are observed when wetting the film. **Figure 1B** shows the effect of the contact with water in the electrospun mat. Here, the UV-vis spectra are compared before (PVA-0 in right scale) and after 30 min in contact with water (PVA-W in left scale). It is observed that the wet mat has a very low absorbance, being consistent with the transparent appearance observed with the naked eye. In both cases, the absorbance is approximately constant in the visible spectrum zone. Then a red laser was chosen to measure the effects of drying time and thickness on the transmittance of the mats over glass slides.

Figure 2, shows the distribution of fiber diameters for different wetting times, obtained from the AFM images. **Table 1** summarizes the average fiber diameters (ϕ) and standard deviations (σ) for each wetting time. As can be observed, ϕ increases with wetting time, revealing the swelling process. The standard deviations remain constant; evidencing that fiber wetting was homogeneous in all cases. It should be noted that there are no significant differences in the diameter of the fibers between the 30 min of wetting and longer times. Therefore, 30 min was

taken as the time for which the maximum swelling is obtained and it was the time that the mats of different thicknesses got wet.

Figure 3 shows the transmittance as a function of the sample thickness taking the drying time as a parameter. Transmittance

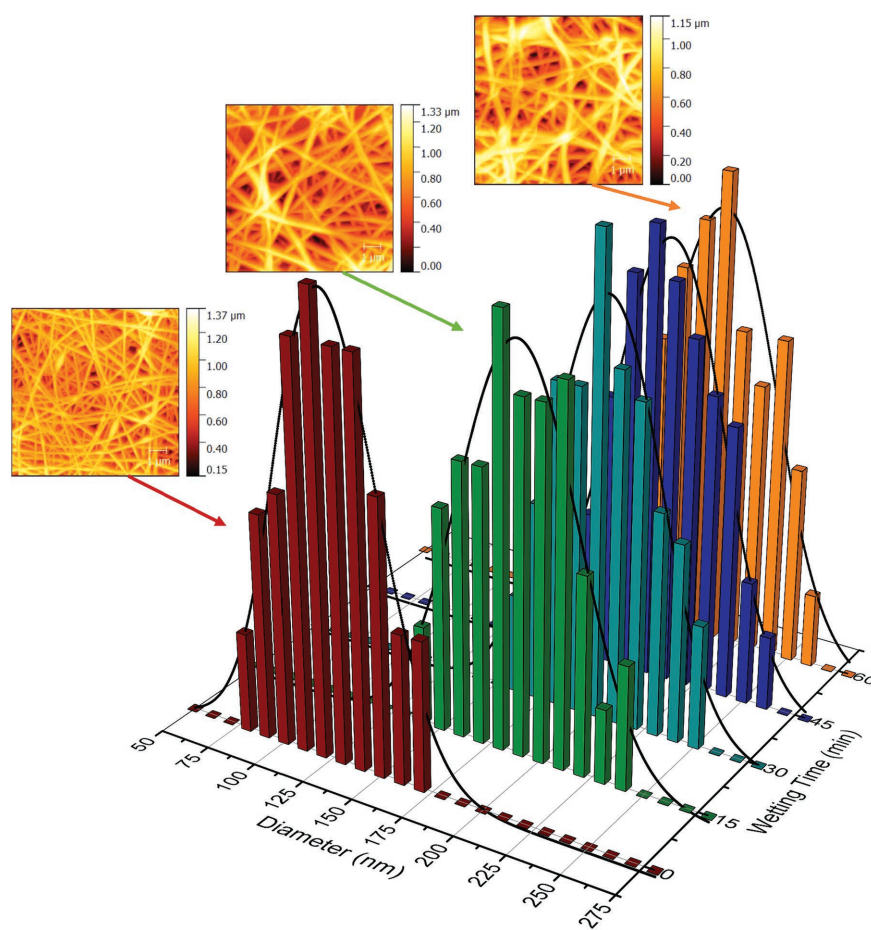


Figure 2. Fiber diameter distributions of electrospun mats for different wetting times and their corresponding AFM images.

Table 1. Mats' wet time and the diameter distribution parameters of electrospun PVA fibers.

Sample name	Wet time [min]	Drying time [days]	Average diameters (φ) [nm]	Standard Deviation of diameters (σ) [nm]
PVA-0	0	0	125 ± 1	26 ± 2
PVA-15	15	0	188 ± 2	28 ± 2
PVA-W	30	0	203 ± 3	27 ± 2
PVA-45	45	0	207 ± 3	28 ± 2
PVA-60	60	0	208 ± 3	29 ± 2
PVA-W+15	30	15	140 ± 2	27 ± 2

values were normalized taking as 1.0 the transmittance of the glass slide used as mat support.

As can be seen in Figure 3, PVA-0 shows a transmittance close to zero for thicknesses greater than or equal to 12 μm . However, for thinner samples, the transmittance increases being 0.37 for a sample of 2 μm thickness. It should be noted that this value is small enough for the mat to look white at naked eye.

The material wet for 30 min without drying time (PVA-W), is much more transparent than PVA-0 for all thicknesses, even 40 μm (see photo in Figure 1). Moreover, the transmittance takes values greater than 0.95 for thicknesses of up to 8 μm and it remains greater than 0.80 for thicknesses between 12 and 28 μm . For larger thicknesses, transmittance decreases up to 0.53 for 40 μm mat. These are consequences of the multiple reflections in the successive layers of mat fibers. Similar effect can be seen in samples having different drying times. As the mats dry out they show transmittances between PVA-0 and PVA-W. However, even after 15 days of drying, the

samples maintain a transmittance much higher than that of PVA-0.

This result agrees with the behavior of the fiber diameter. In Table 1 the average diameter of the fibers is reported, measured by AFM, after 15 days of drying (PVA-W+15). Comparing this value (140 ± 2 nm) with that of the wet sample PVA-W (203 ± 3 nm) it is clear that there is a decrease in the diameter of the fibers as a consequence of water evaporation. However, it does not return to 125 ± 1 nm, that was the average fiber diameter of PVA-0.

Analyzing the transmittance curves (Figure 3), an anomalous effect is observed for the 2 μm thick sample. This, once wet, maintains its transparency, regardless of the drying time. This may be due to an adhesion effect between the mat and the substrate, only observable in very thin samples. If the fibers adhere to the substrate, a continuum is formed between PVA mat and the glass. The refractive index of the PVA is similar to that of glass (1.48 and 1.49, respectively, according to producer) then, total internal reflection does not occur and therefore there are no scattering effects. That is, this material type with this thickness could be used as a water sensor. On the other hand, samples greater than 12 μm show a strong dependence with drying time, which would allow its use as a detector of the elapsed time since the material got wet (drying sensor).

It should be mentioned that the possible effects of waveguide and light coupling to scattered light are negligible compared to the light scattered by the fibers. This is due to the experiment design and to the mat morphology. On the one hand, the light mainly impinges in a perpendicular direction to the mat and on the other hand, fibers have a low surface roughness, are not porous, and are extended throughout the entire sample (i.e., there are no endings of fibers within the observation zone as can be appreciated in Figure S1, Supporting Information).

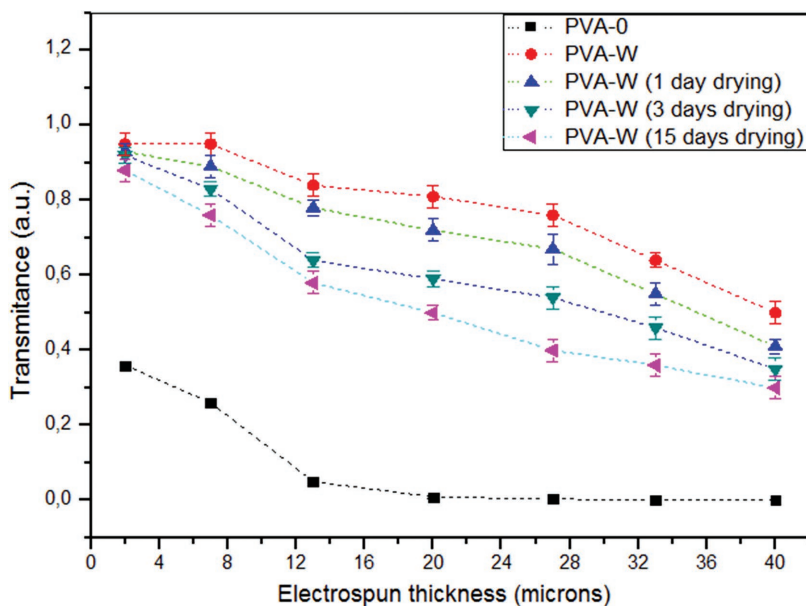


Figure 3. He–Ne laser transmittance of mats before wet (PVA-0), after 30 min wetting (PVA-W), and for different drying times (1, 3, and 15 days). Dotted line is placed only in order to show trend.

The Mie theory of scattering was used to demonstrate that the shift from opaque to transparent, observed in mats after contact with water, is a consequence of changes in fiber diameter and relative refractive index.

Mie solved Maxwell equation for the scattering of optical waves by uniformly distributed particles. An approximation for infinite cylinder, proposed by Bashkatova et al. (2001), has been used to calculate the intensity of light scattering in electrospun nanofibers.^[12] The relevant parameters in this approximation are: the relative refractive index, m (calculated as the ratio between the material refractive index respect to the medium index), and the fiber diameter. The randomly oriented fibers and the mat porosity may be factors to consider when modeling the scattering in electrospun materials. Also, as the fibers absorb water, their flexibility and mobility change modifying the morphology of the whole mat. The sum of these phenomena makes it difficult to obtain a model that predicts quantitatively the electrospun mat. However, a qualitative explanation of the opacity change when the mat is wet can be obtained by using the

Table 2. Parameters used in the law of mixtures to calculate the relative refractive index of samples.

Sample Name	Average fiber diameter (φ) [nm]	PVA fraction f_1	Relative refractive index of PVA contained in fiber m_1	Relative refractive index of water contained in fiber m_2
PVA-0	125 ± 1	1	1.48	–
PVA-W	203 ± 3	0.61	1.11	1
PVA-W+15	140 ± 2	0.80	1.48	1.33

Bashkatova et al. approximation.^[16] For this purpose, the efficiency factor of the scattering was calculated considering the diameter distribution reported in Table 1 and the relative refractive index before and after wetting.

Wetting modifies in two different ways the relative refractive index that presents a fiber. On the one hand, for dry fibers (PVA-0) the surrounding medium is air, while for the wet ones (PVA-W) it is water. On the other hand, while the refractive index of the dry fibers is that of the PVA, when the fiber gets wet it suffers swelling and therefore the water content must be taken into account in the refractive index of the fiber itself. This effect also produces an increase in the diameter of the fiber modifying the scattering factor. The refractive index of the swelled fiber was estimated using the law of mixtures of Equation (1).

$$m = m_1 f_1 + m_2 f_2 \quad (1)$$

where m is the relative refractive index of the mixture, m_1 and m_2 are the relative refractive indexes of the components, f_1 and $f_2 = 1 - f_1$ its volumetric fractions. The values of the constants used for each sample are shown in Table 2.

The volumetric fractions were calculated from the volume ratio of the swollen fibers with respect to the original ones, using the average diameter of Table 1.

It should be noted that if the fiber did not suffer swelling, a change in the refractive index of the medium would change the transparency of the mat anyway. In effect, just a change of air to water changes the m value from 1.48 to 1.11 approaching the m value to 1, which would represent a situation where scattering is not present. However, as PVA suffers swelling when submerged in water, the actual value of m is 1.06. In order to analyze only the effect of the media an experiment was made using a solvent with a similar refractive index to water, but in which PVA does not swell. As a solvent, heptane with a refractive index $n_{\text{heptane}} = 1.39$ was used. The size of the fibers did not change when submerged, as was determined from AFM (see Figure S2, Supporting Information). However, the submerged mat shows transparency with the naked eye (see Figure S3, Supporting Information).

On the other hand, to evaluate only the effect of swelling, the mat could be modeled as a composite material of PVA plus water, surrounded by air. Using the data from Table 2 it was calculated that the m value changes from 1.48 to 1.41. Therefore, both effects contribute with different weights in bringing the relative refractive index nearer to 1 when fibers are in water,

or what is the same, in increasing the transparency of the mat. From this study it is clear that the predominant effect is that of the relationship between the refractive index of the fiber with respect to that of the medium.

The swelling effects have been taken into account for calculating the change in scattering efficiency factor in water using the Bashkatova et al. approximation. The parameters employed in this model are reported in Tables 1 and 2.

The scattering efficiency factor for the wet fiber (PVA-W) results just 0.255% of the dry sample (PVA-0). This result is consistent with the lower transmittance of PVA-0 respect to PVA-W.^[16]

In the case of the fiber dried for 15 days (PVA-W + 15), the efficiency factor of the scattering is 60% of the PVA-0 fibers one, being consistent with the fact that the dried fiber does not recover its initial opacity.

In summary, it was demonstrated that swelling plays a crucial role in the transmittance of the material, leading from opaque to transparent materials when it is wet. This effect strongly depends on the mat thickness. Samples with small thicknesses, of the order of 2 μm , remain transparent (for at least 15 days) after wetting and could act as a water sensor with a persistent response over time. Meanwhile samples with larger thicknesses, greater than or equal to 12 μm , could act as sensors of the time elapsed since the mat got wet for the last time. It should be noted that, even for the thickest sample (40 μm) the transmittance is still 0.50 after 15 days of drying under ambient conditions.

Mat changes from opaque (white) to transparent, were qualitatively explained using the Bashkatova et al. approximation of the Mie theory.

The relevance of swelling effects in the optical properties is not usually taken into account in the literature, even though these have several consequences in the mat industrial application, for example, in its use as optical waveguides, light confinement and propagation, and light-emitting materials, in which the change in diameter and transparency would change its response.

Experimental Section

PVA electrospun mats were fabricated using an environmental friendly methodology from a PVA Mowiol 10–98 solution in water at 12% w/w with 5% (w per PVA weight) of citric acid (CA; Sigma-Aldrich) as a cross-linking agent. PVA solution was placed in a liquid syringe with a 0.9 mm inner diameter steel needle to provide a feed rate of 2.0 mL h⁻¹. The voltage employed was 30 kV and the collection distance was 10 cm. A glass slide that served as the fiber deposition substrate was placed over the collector, which rotates at 1530 ± 10 rpm.

The mat deposition thickness was controlled by the electrospun time, which was pre-calibrated for the PVA solution and process parameters set.

The obtained PVA mats were subjected to a thermal treatment at 190 °C for 10 min in order to cross-link the polymer and avoid its water solubility. Mats with thicknesses between 2 and 40 μm were obtained changing the electrospun time between 5 and 90 min. Four samples of each thickness were made, in order to carry out all the studies in quadruplicate.

The morphology of the initial PVA mat as well as its fiber surface was determined using a high resolution electron microscope (field emission gun FE-SEM; SUPRA 40, Carl Zeiss NTS, Germany). PVA mats

(see Figure S1, Supporting Information) are composed of randomly oriented fibers in a plane parallel to the substrate. Besides, the fiber surfaces are smooth, without pores, even at high magnifications (100k \times). The morphology characteristics shown in Figure S1, Supporting Information, are the typical ones obtained when using a standard electrospinning device. Random fibers are the consequence of the fact that bending instabilities are the dominant effect.^[19] This morphology should be kept in mind when interpreting the results, since a mat with aligned fibers or porosity at single-fiber level could lead to different effects.

To study the water effect on PVA mats morphology an atomic force microscope (AFM; NanoSurf) was used. First AFM images of mat before contact with water (PVA-0) were taken. Then the samples were immersed in water and the morphology was measured at different immersion times (15, 30, 45, and 60 min), in order to study the swelling process. The contact time with water needed to guarantee that the whole sample had suffered the maximum swelling was determined for the thickest sample (40 μm), resulting in 30 min. Once this wetting time was established, all mats were water-immersed for this time (PVA-W) and re-measured 1, 3, and 15 days after wetting, to test the morphological response of the mats to the drying time.

The diameter analysis was made measuring 100 different fibers for each drying condition. It should be mentioned that the sample was mounted in the AFM, before being wet. The time elapsed since the mat was taken out of the water till the AFM measurement was performed, was less than 1 min, which is the AFM alignment time. In all cases a Gaussian distribution of the diameters was obtained from which the mean value and the standard deviation were extracted.

For transmittance measurements, the electrospun mats over glass were mounted on a device consisting of a He–Ne continuous laser (Melles Griot) with a power level of 5 mW. The laser beam impinges perpendicularly in the sample. The power of the transmitted light is measured with a calibrated power meter (Newport) working in the range of the milliwatt with an error 0.001 mW.

Transmittance was determined for the following samples: Mat before contact with water (PVA-0), after 30 min of wetting (PVA-W), and at different drying times (1, 3, and 15 days). The samples thicknesses ranged from 2 to 40 μm . For every given condition (wetting or drying time) four samples were prepared and the transmittance was measured in three different zones. The reported transmittance value is the average of those 12 measurements.

The PVA samples were also immersed in heptane A.C.S. (Ciccarelli) in order to compare the refraction index change with the water immersion experiment. The morphology was measured by AFM to show that in heptane the swelling process does not occur.

Supporting Information

Supporting Information is available from the Wiley Online Library or from the author.

Acknowledgements

This work was supported by the following organizations: CONICET (PIP 2014–2016, 11220120100508CO, and 11220150100475CO), University of Buenos Aires (UBACYT2014–2017, 20020130100495BA, and 20020130100727BA), ANPCyT (PICT-2012-1093, PICT 2016–2940, and

2014–2432). The authors would like to thank Argentine Nanotechnology Foundation FAN for allowing them access to AFM device.

Conflict of Interest

The authors declare no conflict of interest.

Keywords

electrospun nanofibers, Mie scattering, swelling effects

Received: April 19, 2018

Revised: June 19, 2018

Published online:

- [1] S. Goyanes, N. B. D'Accorso, *Industrial Applications of Renewable Biomass Products*, Springer, New York City 2017.
- [2] L. Ribba, M. Parisi, N. B. D'Accorso, S. Goyanes, *J. Biomed. Nanotech.* **2014**, *10*, 12.
- [3] V. Fasano, A. Polini, G. Morello, M. Moffa, A. Camposeo, D. Pisignano, *Macromolecules* **2013**, *46*, 5935.
- [4] Y. Ishii, T. Nobeshima, H. Sakai, K. Omori, S. Uemura, M. Fukuda, *Macromol. Mater. Eng.* **2018**, *303*, 1700302.
- [5] A. Camposeo, M. Gaio, M. Moffa, M. Montinaro, M. Castro-Lopez, V. Fasano, D. Pisignano, *P Soc Photo-opt Ins XIX* **2017**, *10101*, 101010E.
- [6] S. J. Choi, L. Persano, A. Camposeo, J. S. Jang, W. T. Koo, S. J. Kim, H. J. Cho, I. D. Kim, D. Pisignano, *Macromol. Mater. Eng.* **2017**, *302*, 1600569.
- [7] M. Gaio, M. Moffa, M. Castro-Lopez, D. Pisignano, A. Camposeo, R. Sapienza, *ACS Nano* **2016**, *10*, 6125.
- [8] S. Krämmer, C. Vannahme, C. L. Smith, T. Grossmann, M. Jenne, S. Schierle, H. Kalt, *Adv. Mater.* **2014**, *26*, 8096.
- [9] M. Burrelli, L. Cortese, L. Pattelli, M. Kolle, P. Vukusic, D. S. Wiersma, S. Vignolini, *Sci. Rep.* **2014**, *4*, 6075.
- [10] L. Cortese, L. Pattelli, F. Utel, S. Vignolini, M. Burrelli, D. S. Wiersma, *Adv. Opt. Mater.* **2015**, *3*, 1337.
- [11] A. Camposeo, D. Spadaro, D. Magrì, M. Moffa, P. G. Gucciardi, L. Persano, D. Pisignano, *Anal. Bioanal. Chem.* **2016**, *408*, 1357.
- [12] C. C. Chang, C. M. Huang, Y. H. Chang, C. Kuo, *Opt. Express* **2010**, *18*, 102.
- [13] J. M. Corres, Y. R. García, F. J. Arregui, I. R. Matias, *IEEE Sensors J.* **2011**, *11*, 10.
- [14] B. Ding, M. Wang, J. Yu, G. Sun, *IEEE Sensors* **2009**, *9*, 3.
- [15] M. C. Wu, S. H. Chan, T. F. Lin, C. F. Lu, W. F. Su, *J. Taiwan Inst. Chem. Eng.* **2017**, *78*, 552.
- [16] T. A. Bashkatova, A. N. Bashkatov, V. I. Kochubey, V. V. Tuchin, *P. Soc. Photo-Opt. Ins.* **2001**, *4241*, 247.
- [17] A. López-Córdoba, G. R. Castro, S. Goyanes, *Mater. Sci. Eng. C* **2016**, *69*, 726.
- [18] Y. B. Truong, J. Choi, J. Mardel, Y. Gao, S. Maisch, M. Musameh, I. L. Kyratzis, *Macromol. Mater. Eng.* **2017**, *302*, 1700024.
- [19] N. Martínez-Prieto, M. Abecassis, J. Xu, P. Guo, J. Cao, K. F. Ehmman, *J. Micro Nano-Manuf.* **2015**, *3*, 041005.